

Real-Time Reconstruction and Actuation Error Analysis for Markov Sources over MPR Channels

Pansee S. Elessawy and Nikolaos Pappas

Department of Computer and Information Science, Linköping University, Linköping, Sweden

Email: {pansee.elessawy, nikolaos.pappas}@liu.se

Abstract—We study real-time reconstruction and actuation for two binary Markov sources that share a wireless multi-packet reception (MPR) channel. Each sensor follows a stationary randomized sampling policy, and the receiver maintains source estimates using the most recently decoded updates. We derive closed-form expressions for the steady-state real-time reconstruction error (RTE) and the cost of actuation error (CAE) as functions of the source transition probabilities and the effective update probabilities. We then characterize these update probabilities under randomized sampling, linking the physical-layer MPR model to task-oriented reconstruction and actuation metrics. Using these expressions, we formulate a sampling-constrained optimization problem with a weighted-error objective. The resulting analysis reveals how source dynamics, semantic weights, and MPR coupling affect the allocation of sampling resources. Numerical results show that optimized randomized sampling outperforms random, greedy, and time-sharing baselines.

I. INTRODUCTION

Networked autonomous systems, such as industrial automation, connected robotics, and cyber-physical control platforms, rely on timely and accurate information exchange for monitoring and actuation [1], [2]. In such systems, communication should be assessed not only by packet reliability or throughput, but also by its impact on the underlying task [3]–[7].

The Age of Information (AoI) has been widely used to quantify the freshness of status updates at a remote destination [8]–[11]. However, freshness alone does not capture whether the receiver’s estimate is correct, nor the cost incurred when actuation is based on an incorrect estimate. This has motivated beyond-AoI and goal-oriented metrics, such as the Age of Incorrect Information (AoII) [12]–[16], the real-time reconstruction error (RTE), and the cost of actuation error (CAE) [4], [17]. These metrics evaluate information according to its usefulness for real-time reconstruction and actuation.

Goal-oriented sampling for Markov sources has been studied in several settings. Semantics-aware sampling for real-time tracking over an unreliable point-to-point channel was introduced in [3], while CAE minimization under sampling constraints was considered in [18]. Fundamental limits of remote estimation under communication constraints were studied in [19], [20]. In addition, goal-oriented estimation of multiple Markov sources in constrained networks was studied in [21]–[23] and pull-based remote tracking with correlated observations or partial observations in [24]–[26]. AoI has been analyzed in multiple-access systems [27] with multi-packet reception (MPR) [28], and unreliable wireless networks

with scheduling for weighted AoI minimization [29], [30]. Recent works have studied status updating over ALOHA-based random access channels [31], [32]. The works [33], [34] studied two-state Markov source monitoring including joint model estimation with unknown source statistics and analytical renewal–reward characterizations under random and reactive access policies.

In this paper, we study two independent binary Markov sources that share a wireless multiple-access channel with MPR. Unlike collision-based access, MPR allows the receiver to decode more than one simultaneous transmission with nonzero probability [35]. The update probability of each source depends not only on its own sampling decisions, but also on the sampling decisions of the other sensor. *While prior work has mainly studied goal-oriented sampling over point-to-point links or AoI in random access, the role of MPR in real-time reconstruction and actuation has not been thoroughly investigated.*

The main contributions of this paper are as follows. We derive closed-form expressions for the steady-state RTE of binary Markov sources under synchronize-or-hold estimation. We characterize the effective update probabilities induced by stationary randomized sampling over an MPR channel, thereby linking the MPR reception model to the reconstruction and actuation metrics. We obtain the CAE and show that, for binary sources, CAE minimization is equivalent to weighted RTE minimization with modified source weights. Finally, we formulate a sampling-constrained weighted-error minimization problem and study how source dynamics, semantic weights, and MPR coupling affect the allocation of sampling resources.

II. SYSTEM MODEL

We consider a time-slotted remote monitoring system with two sensors, two independent binary Markov sources, and a common receiver communicating over a shared wireless channel with multi-packet reception (MPR), as shown in Fig. 1. Time is indexed by $t \in \{0, 1, 2, \dots\}$. The state of source $i \in \{1, 2\}$ at slot t is denoted by $X_i(t) \in \{0, 1\}$ and evolves according to the transition matrix

$$\mathbf{P}_i = \begin{bmatrix} 1 - \alpha_i & \alpha_i \\ \beta_i & 1 - \beta_i \end{bmatrix}, \quad \alpha_i, \beta_i \in (0, 1), \quad (1)$$

where α_i and β_i are the transition probabilities from 0 to 1 and from 1 to 0, respectively.

At each slot, sensor $k \in \{1, 2\}$ selects an action

$$a_k(t) \in \{0, 1, 2\}, \quad (2)$$

where $a_k(t) = 0$ denotes silence, while $a_k(t) = i$ means that sensor k samples and transmits the current state of source i . We consider the stationary randomized sampling policy

$$\Pr\{a_k(t) = j\} = a_{k,j}, \quad j \in \{0, 1, 2\}, \quad (3)$$

where

$$a_{k,0} + a_{k,1} + a_{k,2} = 1, \quad a_{k,j} \geq 0. \quad (4)$$

The policy of sensor k is denoted by $\mathbf{a}_k \triangleq (a_{k,0}, a_{k,1}, a_{k,2})$ and the joint action by $\mathbf{a}(t) \triangleq (a_1(t), a_2(t))$.

Each transmission occupies one slot. Let $Z_k(t) \in \{0, 1\}$ denote the decoding outcome of sensor k , where $Z_k(t) = 1$ if the packet from sensor k is successfully decoded, otherwise the packet is discarded. The MPR channel is characterized by the success probabilities $p_{1/1}$ and $p_{2/2}$ when sensors 1 and 2 transmit alone, respectively, and by $p_{1/1,2}$ and $p_{2/2,1}$ when both sensors transmit simultaneously. We have $p_{1/1} \geq p_{1/1,2}, p_{2/2} \geq p_{2/2,1}$ ¹.

The receiver maintains an estimate $\hat{X}_i(t) \in \{0, 1\}$ of each source. A successful update for source i occurs if at least one successfully decoded packet carries $X_i(t)$. Thus,

$$U_i(t) \triangleq \mathbf{1}\{(a_1(t) = i, Z_1(t) = 1) \text{ or } (a_2(t) = i, Z_2(t) = 1)\}, \quad i \in \{1, 2\}. \quad (5)$$

The receiver follows a synchronize-or-hold rule

$$\hat{X}_i(t) = \begin{cases} X_i(t), & U_i(t) = 1, \\ \hat{X}_i(t-1), & U_i(t) = 0, \end{cases} \quad i \in \{1, 2\}. \quad (6)$$

The effective update probability of source i is defined as

$$q_i \triangleq \Pr\{U_i(t) = 1\}, \quad i \in \{1, 2\}. \quad (7)$$

We now derive the effective update probabilities defined in (7). Since the sensors select their actions independently under stationary randomized policies, each joint action occurs with probability equal to the product of the corresponding policy probabilities. The effective update probability of source i is then obtained by summing over all joint actions in which at least one successfully decoded packet contains X_i . For source 1, an update occurs in the following cases: sensor 1 transmits X_1 while sensor 2 is silent; sensor 2 transmits X_1 while sensor 1 is silent; both sensors transmit X_1 ; sensor 1 transmits X_1 while sensor 2 transmits X_2 ; or sensor 2 transmits X_1 while sensor 1 transmits X_2 . When both sensors transmit X_1 , the probability that at least one packet is decoded is $1 - (1 - p_{1/1,2})(1 - p_{2/2,1})$.

Thus for $j = 1 + (i \bmod 2), i \in \{1, 2\}$ we have

¹The MPR success probabilities are used as a physical-layer abstraction of the wireless transmission process. In a specific wireless model, these probabilities can be related to channel parameters such as fading statistics, path loss, interference, and decoding threshold [36].

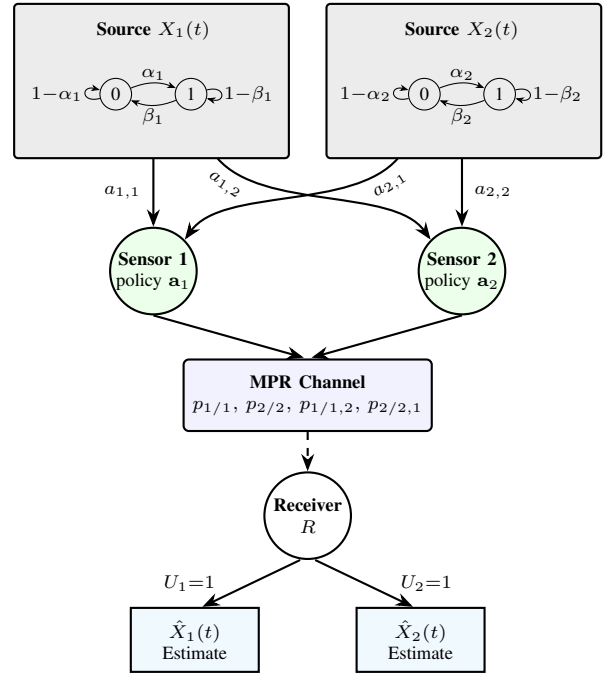


Fig. 1. The considered system model.

$$\begin{aligned} q_i &= a_{1,i}a_{2,0}p_{1/1} + a_{1,0}a_{2,i}p_{2/2} \\ &+ a_{1,i}a_{2,i}\left[1 - (1 - p_{1/1,2})(1 - p_{2/2,1})\right] \\ &+ a_{1,i}a_{2,j}p_{1/1,2} + a_{1,j}a_{2,i}p_{2/2,1}. \end{aligned} \quad (8)$$

III. ANALYSIS

A. Real-Time Reconstruction Error (RTE)

We characterize the reconstruction error by studying the joint evolution of the source $X_i(t)$ and its estimate $\hat{X}_i(t)$. The pair $(X_i(t), \hat{X}_i(t))$ takes values in

$$\mathcal{S} = \{(0, 0), (0, 1), (1, 0), (1, 1)\},$$

with ordering $s_1 = (0, 0)$, $s_2 = (0, 1)$, $s_3 = (1, 0)$, $s_4 = (1, 1)$.

We assume that, within each slot, the source first evolves, and then a successfully decoded update synchronizes the receiver with the current source state; if no update is decoded, the receiver keeps its previous estimate. Under this convention, the joint process $(X_i(t), \hat{X}_i(t))$ is a four-state Markov chain with transition matrix

\mathbf{T}_i , where we define $Y_i(t) \triangleq (X_i(t), \hat{X}_i(t))$. Then

$$T_i(k, \ell) = \Pr\{Y_i(t+1) = s_\ell \mid Y_i(t) = s_k\}. \quad (9)$$

Using (1) and (6), direct enumeration gives

$$\mathbf{T}_i = \begin{bmatrix} 1 - \alpha_i & 0 & \alpha_i(1 - q_i) & \alpha_i q_i \\ q_i(1 - \alpha_i) & (1 - \alpha_i)(1 - q_i) & 0 & \alpha_i \\ \beta_i & 0 & (1 - \beta_i)(1 - q_i) & q_i(1 - \beta_i) \\ \beta_i q_i & \beta_i(1 - q_i) & 0 & 1 - \beta_i \end{bmatrix} \quad (10)$$

For example, from state $(0, 0)$, the process moves to $(1, 0)$ with probability $\alpha_i(1 - q_i)$ when the source changes but no update is received, and to $(1, 1)$ with probability $\alpha_i q_i$ when the source change is followed by a successful update.

Let $\boldsymbol{\pi}_i = [\pi_i(0, 0), \pi_i(0, 1), \pi_i(1, 0), \pi_i(1, 1)]$ denote the stationary distribution of the joint chain. Then

$$\boldsymbol{\pi}_i = \boldsymbol{\pi}_i \mathbf{T}_i, \quad \sum_{(x, \hat{x}) \in \mathcal{S}} \pi_i(x, \hat{x}) = 1. \quad (11)$$

Following [17], the instantaneous reconstruction error is

$$E_i(t) \triangleq \mathbf{1}\{X_i(t) \neq \hat{X}_i(t)\}. \quad (12)$$

Thus, the steady-state real-time reconstruction error (RTE) is

$$E_i \triangleq \Pr(X_i(t) \neq \hat{X}_i(t)) = \pi_i(0, 1) + \pi_i(1, 0). \quad (13)$$

Solving (11) and substituting into (13) yields

$$E_i = \frac{2\alpha_i\beta_i(1 - q_i)}{(\alpha_i + \beta_i)[(\alpha_i + \beta_i) - q_i(\alpha_i + \beta_i - 1)]}. \quad (14)$$

The detailed derivation is omitted due to space limitations but is provided in the online appendix A. Equivalently, defining $\lambda_i \triangleq 1 - \alpha_i - \beta_i$, we obtain

$$E_i = \frac{2\alpha_i\beta_i(1 - q_i)}{(1 - \lambda_i)(1 - \lambda_i(1 - q_i))}. \quad (15)$$

For the two-source system, we consider the weighted reconstruction error

$$E = w_1 E_1 + w_2 E_2, \quad w_1, w_2 \geq 0, \quad (16)$$

where w_i captures the importance of source i .

Remark.

The expression in (14) is stated for $q_i \in (0, 1]$. For $0 < q_i < 1$, the joint Markov chain in (10) is irreducible. If $q_i = 1$, then $E_i = 0$, since the receiver is synchronized in every slot. As $q_i \rightarrow 0$,

$$E_i \xrightarrow{q_i \rightarrow 0} \frac{2\alpha_i\beta_i}{(\alpha_i + \beta_i)^2},$$

which is the mismatch probability between two independent samples drawn from the stationary distribution of $X_i(t)$. When $q_i = 0$, no update is ever received, so $\hat{X}_i(t)$ remains fixed at its initial value and the joint chain is not irreducible. The parameter $\lambda_i = 1 - \alpha_i - \beta_i$ captures the temporal correlation of the source: $\lambda_i > 0$ corresponds to positively correlated dynamics, $\lambda_i = 0$ to the memoryless case, and $\lambda_i < 0$ to negatively correlated dynamics.

Fig. 2 illustrates the effect of (α_i, β_i) on the RTE.

B. Cost of Actuation Error

We next assign costs to the erroneous reconstruction states. Following [17], the generic cost of actuation error (CAE) is

$$\bar{C}_i \triangleq \sum_{x \neq \hat{x}} C_i^{x, \hat{x}} \pi_i(x, \hat{x}), \quad (17)$$

where $C_i^{x, \hat{x}}$ is the cost incurred for source i when the true state is x while the reconstructed state is $\hat{x} \neq x$.

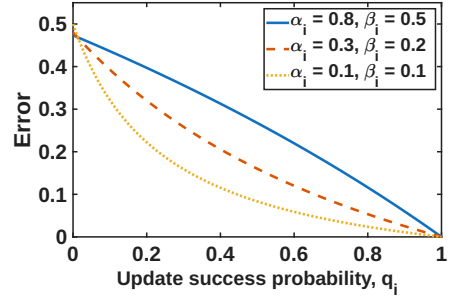


Fig. 2. RTE for different (α_i, β_i) as a function of q_i .

Let $C_i^{0,1}$ and $C_i^{1,0}$ denote the costs of the errors $(X_i, \hat{X}_i) = (0, 1)$ and $(1, 0)$, respectively. Then

$$\bar{C}_i = C_i^{0,1} \pi_i(0, 1) + C_i^{1,0} \pi_i(1, 0). \quad (18)$$

For $q_i > 0$, the stationary balance equations of the four-state chain imply

$$\zeta_i \triangleq \pi_i(0, 1) = \pi_i(1, 0). \quad (19)$$

Therefore,

$$E_i = \pi_i(0, 1) + \pi_i(1, 0) = 2\zeta_i, \quad \zeta_i = \frac{E_i}{2}. \quad (20)$$

Using (14), we obtain

$$\zeta_i = \frac{\alpha_i\beta_i(1 - q_i)}{(\alpha_i + \beta_i)[(\alpha_i + \beta_i) - q_i(\alpha_i + \beta_i - 1)]}, \quad (21)$$

or equivalently, with $\lambda_i \triangleq 1 - \alpha_i - \beta_i$,

$$\zeta_i = \frac{\alpha_i\beta_i(1 - q_i)}{(1 - \lambda_i)(1 - \lambda_i(1 - q_i))}. \quad (22)$$

Substituting (19) into (18) gives

$$\bar{C}_i = (C_i^{0,1} + C_i^{1,0})\zeta_i. \quad (23)$$

Hence,

$$\bar{C}_i = \frac{(C_i^{0,1} + C_i^{1,0})\alpha_i\beta_i(1 - q_i)}{(1 - \lambda_i)(1 - \lambda_i(1 - q_i))}. \quad (24)$$

The weighted total CAE is

$$\bar{C} = w_1 \bar{C}_1 + w_2 \bar{C}_2, \quad w_1, w_2 \geq 0. \quad (25)$$

Remark. Although the directional costs $C_i^{0,1}$ and $C_i^{1,0}$ may be different, the two mismatch states have equal steady-state probabilities under the considered binary Markov model and synchronize-or-hold estimator. Consequently,

$$\bar{C}_i = (C_i^{0,1} + C_i^{1,0})\zeta_i = \frac{C_i^{0,1} + C_i^{1,0}}{2} E_i. \quad (26)$$

Thus, for each binary source under the stationary randomized policies considered here, the CAE is proportional to the corresponding RTE, with proportionality factor $(C_i^{0,1} + C_i^{1,0})/2$. Consequently, weighted CAE minimization is equivalent to weighted RTE minimization with modified source weights. This reduction does not rely on symmetric actuation costs;

it follows from the equality of the two steady-state mismatch probabilities.

For multi-state Markov sources, or for more general dynamic policies whose update decisions depend on the current source state or on the particular mismatch state (X_i, \hat{X}_i) , this simplification does not generally hold, since different mismatch states may have different stationary probabilities.

IV. OPTIMIZATION UNDER SAMPLING CONSTRAINTS

We optimize the stationary randomized sampling policy with respect to the weighted reconstruction objective in (16). For each sensor $k \in \{1, 2\}$, let $\Gamma_k \in (0, 1]$ denote the maximum allowable sampling rate, i.e., the maximum probability with which sensor k is allowed to transmit in a slot. Since transmission occurs whenever action 1 or 2 is selected, the sampling-budget constraint is $a_{k,1} + a_{k,2} \leq \Gamma_k, k \in \{1, 2\}$. The constrained weighted RTE minimization problem is formulated as²

$$\min_{\{a_{k,j}\}} E \quad (27)$$

$$\text{s.t. } a_{k,j} \geq 0, \quad k \in \{1, 2\}, j \in \{0, 1, 2\}, \quad (28)$$

$$a_{k,0} + a_{k,1} + a_{k,2} = 1, \quad k \in \{1, 2\}, \quad (29)$$

$$a_{k,1} + a_{k,2} \leq \Gamma_k, \quad k \in \{1, 2\}. \quad (30)$$

Both objectives depend on the policy through the effective update probabilities $q_i(\mathbf{a}_1, \mathbf{a}_2)$, given by (8). Since these expressions contain bilinear terms of the form $a_{1,j}a_{2,j'}$, the optimization problem in (27) is, in general, nonconvex.

We now derive a structural result for the sampling-constrained problem in (27)–(30). For each sensor $k \in \{1, 2\}$, the feasible policy set is

$$\mathcal{P}_k(\Gamma_k) \triangleq \{\mathbf{a}_k \in \mathbb{R}_{\geq 0}^3 : a_{k,0} + a_{k,1} + a_{k,2} = 1, \\ a_{k,1} + a_{k,2} \leq \Gamma_k\}. \quad (31)$$

Equivalently, since $a_{k,0} = 1 - a_{k,1} - a_{k,2}$, the feasible set in the $(a_{k,1}, a_{k,2})$ plane is the triangular region $a_{k,1} \geq 0, a_{k,2} \geq 0, a_{k,1} + a_{k,2} \leq \Gamma_k$. Then, the extreme points of $\mathcal{P}_k(\Gamma_k)$ are

$$\mathcal{V}_k = \{(1, 0, 0), (1 - \Gamma_k, \Gamma_k, 0), (1 - \Gamma_k, 0, \Gamma_k)\}. \quad (32)$$

The constrained feasible set is $\mathcal{F}_\Gamma = \mathcal{P}_1(\Gamma_1) \times \mathcal{P}_2(\Gamma_2)$.

From (8), each $q_i(\mathbf{a}_1, \mathbf{a}_2)$ is bilinear in the two policy blocks. Hence, for fixed \mathbf{a}_j , it is affine in \mathbf{a}_i . When

$$\lambda_1 \leq 0, \quad \lambda_2 \leq 0, \quad (33)$$

it is straightforward to verify that $E_i(q_i)$ is concave in q_i . Thus, the mappings

$$\mathbf{a}_1 \mapsto E_i(q_i(\mathbf{a}_1, \mathbf{a}_2)), \quad \mathbf{a}_2 \mapsto E_i(q_i(\mathbf{a}_1, \mathbf{a}_2)) \quad (34)$$

²For the binary-source model, the weighted CAE minimization problem has the same feasible set and is equivalent to weighted RTE minimization with modified source weights

$$\tilde{w}_i = w_i \frac{C_i^{0,1} + C_i^{1,0}}{2}, \quad i \in \{1, 2\}.$$

Thus, the results apply to CAE minimization after this weight transformation.

are concave in each block. Consequently,

$$E(\mathbf{a}_1, \mathbf{a}_2) = w_1 E_1(q_1(\mathbf{a}_1, \mathbf{a}_2)) + w_2 E_2(q_2(\mathbf{a}_1, \mathbf{a}_2)) \quad (35)$$

is concave in \mathbf{a}_1 for fixed \mathbf{a}_2 , and concave in \mathbf{a}_2 for fixed \mathbf{a}_1 .

Theorem 1: If $\lambda_1 \leq 0$ and $\lambda_2 \leq 0$, then at least one global minimizer of the sampling-constrained RTE problem over \mathcal{F}_Γ is attained at a pair of constrained vertices. Equivalently,

$$E^* = \min_{\mathbf{v}_1 \in \mathcal{V}_1, \mathbf{v}_2 \in \mathcal{V}_2} E(\mathbf{v}_1, \mathbf{v}_2). \quad (36)$$

Thus, a global optimum can be found by evaluating only nine candidate policy pairs.

Proof: Fix $\mathbf{a}_2 \in \mathcal{P}_2(\Gamma_2)$. Since $E(\mathbf{a}_1, \mathbf{a}_2)$ is concave in \mathbf{a}_1 , it admits at least one minimizer over the compact convex polytope $\mathcal{P}_1(\Gamma_1)$ at an extreme point. Hence,

$$\min_{\mathbf{a}_1 \in \mathcal{P}_1(\Gamma_1)} E(\mathbf{a}_1, \mathbf{a}_2) = \min_{\mathbf{v}_1 \in \mathcal{V}_1} E(\mathbf{v}_1, \mathbf{a}_2). \quad (37)$$

For each fixed $\mathbf{v}_1 \in \mathcal{V}_1$, the function $E(\mathbf{v}_1, \mathbf{a}_2)$ is concave in \mathbf{a}_2 . Therefore, it admits at least one minimizer over $\mathcal{P}_2(\Gamma_2)$ at an extreme point

$$\min_{\mathbf{a}_2 \in \mathcal{P}_2(\Gamma_2)} E(\mathbf{v}_1, \mathbf{a}_2) = \min_{\mathbf{v}_2 \in \mathcal{V}_2} E(\mathbf{v}_1, \mathbf{v}_2). \quad (38)$$

Combining (37) and (38) proves (36). ■

For example, the constrained vertex pair

$$\mathbf{v}_1 = (1 - \Gamma_1, \Gamma_1, 0), \quad \mathbf{v}_2 = (1, 0, 0)$$

corresponds to sensor 1 using its full budget for source 1 while sensor 2 remains silent, and gives $(q_1, q_2) = (\Gamma_1 p_{1/1}, 0)$. Similarly, the vertex pair

$$\mathbf{v}_1 = (1 - \Gamma_1, \Gamma_1, 0), \quad \mathbf{v}_2 = (1 - \Gamma_2, 0, \Gamma_2)$$

corresponds to sensor 1 allocating its full budget to source 1 and sensor 2 allocating its full budget to source 2. In this case,

$$q_i = \Gamma_i(1 - \Gamma_j)p_{i/i} + \Gamma_i\Gamma_j p_{i/i,j}, \\ j = 1 + (i \bmod 2), \quad i \in \{1, 2\}. \quad (39)$$

The remaining seven candidates are obtained by substituting all pairs $(\mathbf{v}_1, \mathbf{v}_2) \in \mathcal{V}_1 \times \mathcal{V}_2$ into (8). Thus, under (33), the constrained optimization reduces to evaluating $E(\mathbf{v}_1, \mathbf{v}_2)$ over the nine vertex pairs in $\mathcal{V}_1 \times \mathcal{V}_2$.

Remark. In this regime $\lambda_i \leq 0$, the per-source error functions are concave in the update probabilities, and at least one constrained vertex policy is globally optimal. When at least one λ_i is positive, this concavity is lost and an interior randomized policy may become optimal. This case is omitted due to space limitations.

V. NUMERICAL RESULTS AND DISCUSSION

In this section, we evaluate the optimized stationary randomized policy. We compare the optimized policy with four baselines: (i) a *random policy*, where each sensor splits its sampling budget uniformly between the two sources; (ii) *Greedy Source 1*, where both sensors allocate their entire available budget to source X_1 ; (iii) *Greedy Source 2*,

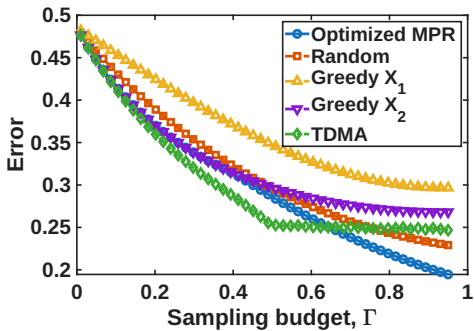


Fig. 3. Total reconstruction error versus sampling budget Γ .

where both sensors allocate their entire available budget to source X_2 ; and (iv) a *time-division multiple access (TDMA) policy*³, where the sensors are orthogonalized in time so that at most one sensor transmits in each slot. When scheduled, sensor i uses its available sampling budget to transmit source X_i .

A. Impact of the Sampling Budget

Fig. 3 shows the total reconstruction error E as a function of the common sampling budget Γ . We use $(\alpha_1, \beta_1) = (0.8, 0.6)$, $(\alpha_2, \beta_2) = (0.3, 0.2)$, representing a highly dynamic source and a moderately dynamic source, respectively. The MPR parameters are $p_{1/1} = 0.9$, $p_{2/2} = 0.85$, $p_{1/1,2} = 0.6$, $p_{2/2,1} = 0.55$, with weights $w_1 = w_2 = 0.5$ and $\Gamma \in [0.01, 0.95]$.

As expected, increasing Γ reduces E for all policies, since more frequent sampling increases the update probabilities. The optimized policy achieves a consistently lower reconstruction error than the random and greedy baselines, especially at moderate and large budgets. This shows that allocating all resources to a single source is generally suboptimal when the sources have different dynamics and the update probabilities are coupled through the MPR channel. Instead, the optimized policy balances the sampling resources across sources according to their dynamics, channel reliability, and contribution to the weighted reconstruction error.

The comparison with TDMA illustrates the role of simultaneous transmissions. At low sampling budgets, TDMA is advantageous because scarce transmission opportunities avoid interference. At high budgets, however, the MPR policy becomes superior because simultaneous transmissions can be exploited to deliver multiple updates within the same slot, rather than restricting transmissions through strict orthogonalization.

B. Effect of Semantic Weights

We next study the effect of the semantic weight w_2 on the optimized policy, with $w_1 = 1 - w_2$. The parameters

³In the TDMA baseline, at most one sensor is allowed to transmit in each slot. We optimize over the long-term time fractions $\tau_{11}, \tau_{12}, \tau_{21}, \tau_{22}$, where τ_{ki} denotes the fraction of slots in which sensor k transmits source i . The same per-sensor sampling budgets are used as in the MPR case, i.e., $\tau_{11} + \tau_{12} \leq \Gamma_1$ and $\tau_{21} + \tau_{22} \leq \Gamma_2$, with the additional TDMA orthogonality constraint $\tau_{11} + \tau_{12} + \tau_{21} + \tau_{22} \leq 1$. The time fractions are optimized and are not fixed to an equal split in order to achieve better performance.

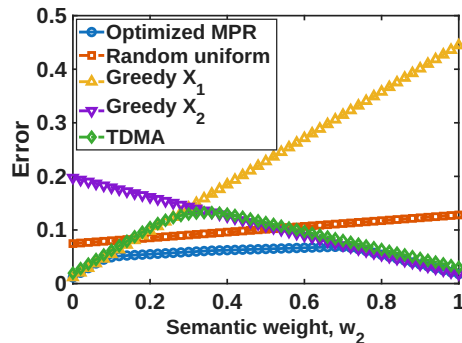


Fig. 4. Total reconstruction error $E(w_2)$ versus semantic weight.

are $(\alpha_1, \beta_1) = (0.8, 0.1)$, $(\alpha_2, \beta_2) = (0.4, 0.2)$, and $p_{1/1} = 0.9$, $p_{2/2} = 0.85$, $p_{1/1,2} = 0.82$, $p_{2/2,1} = 0.78$. Both sensors satisfy $\Gamma_1 = \Gamma_2 = 0.9$.

Fig. 4 shows that the optimized policy adapts to the semantic priority of the sources. When w_2 is small, the objective is dominated by source 1, and the optimized performance approaches the Greedy Source 1 baseline. As w_2 increases, the policy reallocates sampling resources toward source 2. In the intermediate regime, the optimized curve exhibits a mild non-monotonic behavior, reflecting the tradeoff between source dynamics, semantic weights, and MPR coupling. Unlike the greedy baselines, which commit the sampling budget to one source, the optimized randomized policy balances the two sources and achieves the lowest reconstruction error over the considered range.

The TDMA curve lies between the two greedy baselines because it orthogonalizes transmissions while allocating time across the sources.

In this strong-MPR regime, TDMA is less efficient because it prevents simultaneous transmissions that could otherwise be decoded reliably. Hence, with high sampling budgets, MPR better exploits the channel by allowing concurrent updates, leading to lower reconstruction error.

VI. CONCLUSION

This paper studied real-time reconstruction and actuation for two binary Markov sources sharing an MPR channel. We derived closed-form expressions for the RTE and CAE in terms of the source dynamics and the effective update probabilities, and characterized how these update probabilities depend on the stationary randomized sampling policy and the MPR reception model. For binary sources, we showed that CAE minimization is equivalent to weighted RTE minimization with modified source weights. We then formulated a sampling-constrained weighted-error minimization problem and identified a source-dynamics regime in which a constrained vertex policy is globally optimal. Numerical results showed that optimized randomized policies outperform random, greedy, and time-sharing baselines, and highlighted the impact of source dynamics, channel conditions, semantic weights, and MPR coupling on

sampling-resource allocation. Future work may consider larger setups, and adaptive sampling policies.

APPENDIX

In this appendix, we provide the algebraic steps leading to the closed-form expression of the steady-state real-time reconstruction error in (14).

Let

$$\pi_{00} \triangleq \pi_i(0, 0), \quad \pi_{01} \triangleq \pi_i(0, 1),$$

$$\pi_{10} \triangleq \pi_i(1, 0), \quad \pi_{11} \triangleq \pi_i(1, 1).$$

so that $\boldsymbol{\pi}_i = [\pi_{00}, \pi_{01}, \pi_{10}, \pi_{11}]$.

From the stationary condition $\boldsymbol{\pi}_i = \boldsymbol{\pi}_i \mathbf{T}_i$

and the transition matrix in (10), the balance equations corresponding to the two mismatch states (0, 1) and (1, 0) are

$$\pi_{01} = (1 - q_i)[(1 - \alpha_i)\pi_{01} + \beta_i\pi_{11}], \quad (40)$$

$$\pi_{10} = (1 - q_i)[\alpha_i\pi_{00} + (1 - \beta_i)\pi_{10}]. \quad (41)$$

Next, note that the marginal distribution of $X_i(t)$ must coincide with the stationary distribution of the underlying binary Markov source. Hence,

$$\pi_{00} = \frac{\beta_i}{\alpha_i + \beta_i} - \pi_{01}, \quad \pi_{11} = \frac{\alpha_i}{\alpha_i + \beta_i} - \pi_{10}. \quad (42)$$

Substituting (42) into (40) gives

$$[1 - (1 - q_i)(1 - \alpha_i)]\pi_{01} + \beta_i(1 - q_i)\pi_{10} = \frac{\alpha_i\beta_i(1 - q_i)}{\alpha_i + \beta_i}. \quad (43)$$

Similarly, substituting (42) into (41) yields

$$\alpha_i(1 - q_i)\pi_{01} + [1 - (1 - q_i)(1 - \beta_i)]\pi_{10} = \frac{\alpha_i\beta_i(1 - q_i)}{\alpha_i + \beta_i}. \quad (44)$$

Subtracting (44) from (43), we obtain

$$q_i(\pi_{01} - \pi_{10}) = 0, \quad (45)$$

which implies

$$\pi_{01} = \pi_{10}. \quad (46)$$

Let

$$\zeta_i \triangleq \pi_{01} = \pi_{10}.$$

Substituting (46) into (43) gives

$$(1 - (1 - q_i)(1 - \alpha_i) + \beta_i(1 - q_i))\zeta_i = \frac{\alpha_i\beta_i(1 - q_i)}{\alpha_i + \beta_i}.$$

Finally, since $E_i = \pi_{01} + \pi_{10} = 2\zeta_i$, we obtain

$$E_i = \frac{2\alpha_i\beta_i(1 - q_i)}{(\alpha_i + \beta_i)[(\alpha_i + \beta_i) - q_i(\alpha_i + \beta_i - 1)]}. \quad (47)$$

REFERENCES

- [1] S. Vitturi, F. Tamarin, and L. Seno, "Industrial wireless networks: The significance of timeliness in communication systems," *IEEE Industrial Electronics Magazine*, vol. 7, no. 2, pp. 40–51, 2013.
- [2] J. Gielis, A. Shankar, and A. Prorok, "A critical review of communications in multi-robot systems," *Current robotics reports*, vol. 3, no. 4, pp. 213–225, 2022.
- [3] N. Pappas and M. Kountouris, "Goal-oriented communication for real-time tracking in autonomous systems," in *IEEE International Conference on Autonomous Systems (ICAS)*, 2021.
- [4] J. Luo, E. Delfani, M. Salimnejad, and N. Pappas, "From information freshness to semantics of information and goal-oriented communications," *arXiv preprint arXiv:2512.12758*, 2025.
- [5] P. Popovski, O. Simeone, F. Boccardi, D. Gündüz, and O. Sahin, "Semantic-effectiveness filtering and control for post-5g wireless connectivity," *Journal of the Indian Institute of Science*, vol. 100, no. 2, pp. 435–443, 2020.
- [6] E. Calvanese Strinati and S. Barbarossa, "6g networks: Beyond shannon towards semantic and goal-oriented communications," *Computer Networks*, vol. 190, p. 107930, 2021.
- [7] E. Uysal, O. Kaya, A. Ephremides, J. Gross, M. Codreanu, P. Popovski, M. Assaad, G. Liva, A. Munari, B. Soret, T. Soleymani, and K. H. Johansson, "Semantic communications in networked systems: A data significance perspective," *IEEE Network*, vol. 36, no. 4, pp. 233–240, 2022.
- [8] S. Kaul, R. Yates, and M. Gruteser, "Real-time status: How often should one update?" in *IEEE INFOCOM*, 2012.
- [9] A. Kosta, N. Pappas, and V. Angelakis, "Age of information: A new concept, metric, and tool," *Foundations and Trends in Networking*, vol. 12, no. 3, pp. 162–259, 2017.
- [10] R. D. Yates, Y. Sun, D. R. Brown, S. K. Kaul, E. Modiano, and S. Ulukus, "Age of information: An introduction and survey," *IEEE Journal on Selected Areas in Communications*, vol. 39, no. 5, pp. 1183–1210, 2021.
- [11] Y. Sun, E. Uysal-Biyikoglu, R. D. Yates, C. E. Koksal, and N. B. Shroff, "Update or wait: How to keep your data fresh," *IEEE Transactions on Information Theory*, vol. 63, no. 11, pp. 7492–7508, 2017.
- [12] A. Maatouk, S. Kriouile, M. Assaad, and A. Ephremides, "The age of incorrect information: A new performance metric for status updates," *IEEE/ACM Transactions on Networking*, vol. 28, no. 5, pp. 2215–2228, 2020.
- [13] I. Cosandal, N. Akar, and S. Ulukus, "Multi-threshold aoi-optimum sampling policies for continuous-time markov chain information sources," *IEEE Transactions on Information Theory*, vol. 71, no. 9, pp. 6968–6988, 2025.
- [14] A. Maatouk, M. Assaad, and A. Ephremides, "The age of incorrect information: An enabler of semantics-empowered communication," *IEEE Transactions on Wireless Communications*, vol. 22, no. 4, pp. 2621–2635, 2023.
- [15] C. Kam, S. Kompella, and A. Ephremides, "Age of incorrect information for remote estimation of a binary markov source," in *IEEE Conference on Computer Communications Workshops*, 2020.
- [16] I. Cosandal, N. Akar, and S. Ulukus, "Modeling aoi in push- and pull-based sampling of continuous time markov chains," in *IEEE Conference on Computer Communications Workshops*, 2024.
- [17] M. Salimnejad, M. Kountouris, and N. Pappas, "Real-time reconstruction of markov sources and remote actuation over wireless channels," *IEEE Transactions on Communications*, vol. 72, no. 5, pp. 2701–2715, 2024.
- [18] E. Fountoulakis, N. Pappas, and M. Kountouris, "Goal-oriented policies for cost of actuation error minimization in wireless autonomous systems," *IEEE Communications Letters*, vol. 27, no. 9, 2023.
- [19] J. Chakravorty and A. Mahajan, "Fundamental limits of remote estimation of autoregressive markov processes under communication constraints," *IEEE Transactions on Automatic Control*, vol. 62, no. 3, pp. 1109–1124, 2017.
- [20] Y. Sun, Y. Polyanskiy, and E. Uysal, "Sampling of the wiener process for remote estimation over a channel with random delay," *IEEE Transactions on Information Theory*, vol. 66, no. 2, pp. 1118–1135, 2020.
- [21] J. Luo and N. Pappas, "Semantic-aware remote estimation of multiple markov sources under constraints," *IEEE Transactions on Communications*, 2025.

- [22] M. Salimnejad, M. Kountouris, and N. Pappas, "Real-time remote monitoring of correlated markovian sources," *IEEE Open Journal of the Communications Society*, vol. 7, pp. 2777–2793, 2026.
- [23] N. Akar and S. Ulukus, "Query-based sampling of heterogeneous ctmc: Modeling and optimization with binary freshness," *IEEE Transactions on Communications*, vol. 72, no. 12, pp. 7705–7714, 2024.
- [24] A. Zakeri, M. Moltafet, and M. Codreanu, "Goal-oriented remote tracking through correlated observations in pull-based communications," *IEEE Communications Letters*, vol. 29, no. 12, pp. 2805–2809, 2025.
- [25] I. Cosandal, S. Ulukus, and N. Akar, "Which sensor to observe? timely tracking of a joint markov source with model predictive control," in *IEEE International Symposium on Information Theory*, 2025, pp. 1–6.
- [26] F. Chiarriotti, J. Holm, A. E. Kalør, B. Soret, S. K. Jensen, T. B. Pedersen, and P. Popovski, "Query age of information: Freshness in pull-based communication," *IEEE Transactions on Communications*, vol. 70, no. 3, pp. 1606–1622, 2022.
- [27] R. D. Yates and S. K. Kaul, "Status updates over unreliable multiaccess channels," in *IEEE International Symposium on Information Theory (ISIT)*, 2017, pp. 331–335.
- [28] Z. Chen, N. Pappas, E. Björnson, and E. G. Larsson, "Optimizing information freshness in a multiple access channel with heterogeneous devices," *IEEE Open Journal of the Communications Society*, vol. 2, pp. 456–470, 2021.
- [29] I. Kadota, A. Sinha, E. Uysal-Biyikoglu, R. Singh, and E. Modiano, "Scheduling policies for minimizing age of information in broadcast wireless networks," *IEEE/ACM Transactions on Networking*, vol. 26, no. 6, pp. 2637–2650, 2018.
- [30] I. Kadota, A. Sinha, and E. Modiano, "Scheduling algorithms for optimizing age of information in wireless networks with throughput constraints," *IEEE/ACM Transactions on Networking*, vol. 27, no. 4, pp. 1359–1372, 2019.
- [31] A. Munari, "Modern random access: An age of information perspective on irregular repetition slotted aloha," *IEEE Transactions on Communications*, vol. 69, no. 6, pp. 3572–3585, 2021.
- [32] F. Zhao, N. Pappas, C. Ma, X. Sun, T. Q. S. Quek, and H. H. Yang, "Age-threshold slotted aloha for optimizing information freshness in mobile networks," *IEEE Transactions on Wireless Communications*, vol. 23, no. 11, pp. 17 236–17 251, 2024.
- [33] H. Asgari, A. Munari, G. Liva, and G. Cocco, "Remote monitoring of two-state markov sources in random access channels: Joint model and state estimation," in *14th International ITG Conference on Systems, Communications and Coding (SCC)*, 2025.
- [34] H. Asgari, G. Cocco, and A. Munari, "Random-access monitoring of markov sources: Analytical characterization of uncertainty," in *IEEE ISIT*, 2026.
- [35] S. Ghez, S. Verdu, and S. Schwartz, "Stability properties of slotted aloha with multipacket reception capability," *IEEE Transactions on Automatic Control*, vol. 33, no. 7, pp. 640–649, 1988.
- [36] V. Naware, G. Mergen, and L. Tong, "Stability and delay of finite-user slotted aloha with multipacket reception," *IEEE Transactions on Information Theory*, vol. 51, no. 7, pp. 2636–2656, 2005.